Accepted Manuscript

Ion Exchange Homogeneous Surface Diffusion Modelling by Binary Site Resin for the Removal of Nickel Ions from Wastewater in Fixed Beds

Anthony Ma, Ahmed Abushaikha, Stephen J. Allen, Gordon McKay

PII: S1385-8947(18)31847-3
DOI: https://doi.org/10.1016/j.cej.2018.09.135
Reference: CEJ 19974

To appear in: *Chemical Engineering Journal*

Received Date: 17 February 2018
Revised Date: 15 September 2018
Accepted Date: 17 September 2018

Please cite this article as: A. Ma, A. Abushaikha, S.J. Allen, G. McKay, Ion Exchange Homogeneous Surface Diffusion Modelling by Binary Site Resin for the Removal of Nickel Ions from Wastewater in Fixed Beds, *Chemical Engineering Journal* (2018), doi: https://doi.org/10.1016/j.cej.2018.09.135

This is a PDF file of an unedited manuscript that has been accepted for publication. As a service to our customers we are providing this early version of the manuscript. The manuscript will undergo copyediting, typesetting, and review of the resulting proof before it is published in its final form. Please note that during the production process errors may be discovered which could affect the content, and all legal disclaimers that apply to the journal pertain.

ACCEPTED MANUSCRIPT

Ion Exchange Homogeneous Surface Diffusion Modelling by Binary Site Resin for the Removal of Nickel Ions from Wastewater in Fixed Beds

Anthony Ma[1,2], Ahmed Abushaikha[3], Stephen J. Allen[4] and Gordon McKay[3,*]

[1]Hong Kong Productivity Council, Tat Chee Avenue, Kowloon, Hong Kong

[2]Department of Chemical and Bimolecular Engineering, Hong Kong University of Science and Technology, Clear Water Bay, Kowloon, Hong Kong

[3]Division of Sustainable Development, College of Science and Engineering, Hamad Bin Khalifa University, Education City, Qatar Foundation, Doha, Qatar

[4]School of Chemistry and Chemical Engineering, The Queen's University of Belfast, Belfast, Northern Ireland.

*Corresponding Author Email: gmckay@qf.org.qa

ACCEPTED MANUSCRIPT

ACCEPTED MANUSCRIPT

Abstract

The presence of toxic heavy metals in wastewater is a continuing threat to both the environment and living organisms. The present study investigates the ion-exchange potential of a dual-exchanged (Na+/H+) chelating resin to remove nickel ions from wastewater in a fixed bed column ion exchanger. The resin contains iminodiacetic acid (IDA) functional groups that can lead to the capture of heavy metal ions, provided that the pH condition and ratio of Na^+: H^+ are appropriate. Too much Na^+ results in precipitation of nickel hydroxide, resulting in clogging of the ion exchange columns, while too much H^+ in the solution leads to competitive protonation, reducing the uptake of Ni^{2+} ions. The experimental work has been supported by modelling results using a new film-homogeneous surface diffusion model (HSDM) to simulate the fixed bed breakthrough curves for the two exchange processes – assigned 1 and 2. The best fit model simulation curves were obtained by optimizing the overall external diffusion mass transfer coefficient k_f (= 5.41 x 10^{-3} cms^{-1}), the surface diffusivity D_s (D_{s1} = 224 x $10^{-7}cm^2s^{-1}$ for $2Na^+/ Ni^{2+}$ exchange; and, D_{s2} = 3.60 x 10^{-10} cm^2s^{-1} for $2H^+/ Ni^{2+}$ exchange) and the equilibrium constant K_{RP} (K_{RP1} = 351 dm^3/g for $2Na^+/ Ni^{2+}$ exchange; and K_{RP2} = 781 dm^3/g for $2H^+/ Ni^{2+}$ exchange) until a good fit was obtained between the model and experimental data. Optimisation was achieved by employing the downhill simplex method and performing a multidimensional minimization of the objective function, i.e. minmizing the SSE between the experimental data and the model prediction.

Keywords: Nickel ions removal; iminodiacetate resin; fixed bed ion exchange; binary-site surface diffusion modelling; breakthrough curves.

ACCEPTED MANUSCRIPT

1.0 Introduction

Industries, such as the microelectronics, printed circuit board manufacturing, coin production and metal finishing, discharge large quantities of metal-bearing waste effluents, which become a major environmental problem. A significant issue of these toxic heavy metals is their ability to wipe out microbial cultures in wastewater and sewage treatment plants [1,2].

Toxic metals, like copper, nickel and zinc, are most commonly found in waste effluents with the result that governments continue to tighten the environmental discharge and exposure regulations [3,4]. Heavy metal contamination of water bodies is a serious issue as metal in drinking water can cause chronic or acute diseases to humans. Bioaccumulation of heavy metals can occur in fish or agriculture, and humans at the highest food chain level, which will receive all of the heavy metals across the food chain creating the highest health risk. The metal, nickel, studied in the present work, is known to cause dermatitis and eczema, and is a recognised carcinogen responsible for lung and bone cancer [5-7].

Ion exchange is a technique that can separate dissolved ions from the water and has been used for the production of high purity water. Since ion exchange resins have a very strong affinity for dissolved ions, including heavy metals, ion exchange is highly suitable in purifying waste effluent to comply with the most stringent environmental discharge standards. Nevertheless, until the emergence of chelating ion exchange resins, the purification of electroplating effluents using common ion exchange resins was not economic due to the rapid saturation of the ion exchange resins. The emergence of chelating resins has allowed metal ions to be recovered

ACCEPTED MANUSCRIPT

selectively from waste water. This has made the application of ion exchange for metal removal in wastewater treatment increasingly popular [8].

Chelating ion exchange resins are, in general, copolymers with covalently bonded side chains that can form coordinate bonds with most of the toxic metal ions [9,10]. The amino groups are well established as groups that provide nitrogen lone pair electrons for ions to form covalent bonds [11,12]. Due to coordination-type interactions, all such chelating exchangers offer extremely high selectivity toward commonly encountered toxic divalent cations, namely Cu^{2+}, Pb^{2+}, Ni^{2+},Cd^{2+} and Zn^{2+}, over competing alkaline (Na^{+}, K^{+}) and alkaline-earth (Ca^{2+}, Mg^{2+}) metal cations[13]. Waste derived exchangers [12,14] and polymerHIPE membranes [15] have demonstrated high removal capacities for nickel and cobalt.

Chelating resins with iminodiacetic acid (IDA) functional groups are one of the best known chelating resins for heavy metal removal and recovery. Each IDA functional group contains one nitrogen atom and two carboxylic groups with Na^{+} or H^{+} oxygen atoms as the donor atoms, which can form coordinate bonds with the heavy metal ion. The two carboxylic groups contain Na+ or H+ ions for direct ion exchange. A divalent metal ion can strongly exchange with two of these donor atoms to the IDA functional group. Therefore, IDA type chelating resins are now widely used in many industrial applications for wastewater treatment and metal recovery. Dabrowski et al. [16] produced a comprehensive review on the selective removal of heavy metal ions from the wastewater by ion exchange method.

From literature, several research studies on heavy metals removal by the IDA chelating resins have been conducted by the various workers. The equilibrium and

ACCEPTED MANUSCRIPT

activity coefficients in metal-iminodiacetate resin were studied and determined by Fernandez *et al.* [17]. Binary metal equilibrium data were obtained at different temperatures and ionic strengths, and two sets of ternary systems: close selectivity (Zn^{2+}, Co^{2+} and Na^{+}) and distinct selectivity (Cu^{2+}, Co^{2+} and Na^{+}) were also studied for the IDA chelating resin by Arevalo *et al.* [18]. Pesavento *et al.* [19] applied the Gibbs-Donnan model to describe and predict the metal sorption in IDA chelating resin. Malla *et al.* [20] evaluated the sorption and desorption characteristics of Cd, Pb and Zn on the IDA chelating resin, while Kargman *et al.* [21] studied the selectivity of IDA chelating resins for heavy metals in the electroplating wastewater. Koivula *et al*. [22] tested a wide range of chelating ion exchangers for their abilities to remove heavy metals from metal plating rinse waters.

As the IDA functional group of the chelating resins is a weak acid, all of the IDA chelating resins exhibit high affinity toward hydrogen ions. This process is called protonation. Due to the protonation effect, the ion exchange capacity will reduce in an acidic environment. Mijangos and Diaz [23] studied the pH effects on the capacity of Cu, Ni, Zn and Co in the IDA chelating resin and found that the resin capacity decreased with decreasing pH below 4. On the other hand, hydrolysis of the chelating resin takes place when the hydrogen ion produced in the autoprotolysis of water exchanges with the counter-ions, like Na^{+}, loaded in the resin. Thus, Leinonen and Lehto [24] demonstrated how an IDA chelating resin behaved as a multi-component (H-Na-divalent metal) ion-exchange system and explained how the pH changed due to the hydrolysis of the resin and protonation during the batch equilibrium studies with divalent metal ions.

ACCEPTED MANUSCRIPT

Wolowicz and Hubicki [25] used chelating resin for noble metals Pd, Pt and Au and for some basic metals Cu, Co, Ni and Zn. Good ion exchange capacities were achieved for the three noble metals but the base metals were removed to a much lower extent. The removal of nickel using amine chelating ion exchange resin was enhanced by over 50% by the addition of the salts NaCl and $CaCl_2$ [26].

Although fixed bed systems employing chelating ion exchange resin have been applied to remove toxic heavy metals from the industrial wastewater for years, the design of industrial ion exchange systems has traditionally relied on pilot studies to gain the required information to predict column behavior in full scale treatment plants with various design and operating parameters. Pilot studies are relatively expensive and time consuming. Mathematical process models [27,28] can facilitate the design of full-scale systems simply by reducing the number of pilot-scale tests required to evaluate various operating conditions and design parameters.

The present study involves the removal of nickel ions from wastewater using a series of fixed bed experiments and an iminodiacetate ion exchange resin. A homogeneous surface diffusion model has been developed to simulate the experimental breakthrough curves by optimizing the key major design parameters:- the external diffusion coefficient, the surface diffusivity and the isotherm equilibrium constant. These parameters describe the ion exchange process, which can then be used to design systems using this resin.

ACCEPTED MANUSCRIPT

2.0 Experimental Program

2.1 Materials

2.1.1 Chelating Ion Exchange Resin

The iminodiacetate chelating resin sample is Suqing D401 (D401 in short) which is produced by the Jiang Yin Organic Chemical Company, China. The resins have the iminodiacetate functional group and the initial ionic forms are di-hydrogen before being converted into a di-sodium form or a composite resin of di-Na and di-H, by conditioning with NaOH.

The structure and physical characteristics of the chelating resin is shown in Figure 1 and Table 1 respectively.

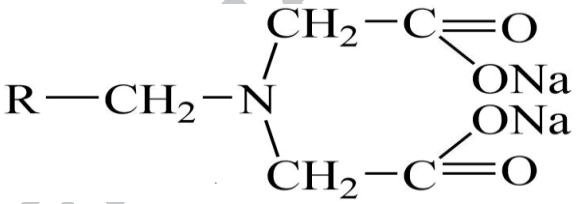

Figure 1. Structure of iminodiacetate chelating resin

Table 1 Physical Properties of D401

Functional group	Iminodiacetate
Ionic form	Sodium
Appearance	Opaque spheres
Bulk density, g/l	700 – 800
Particle density, g/l	1150 – 1250
Water retention, %	50 – 60
Particle size, mm	0.4 – 1.25 (>=95%)
Maximum operating temperature, ^{o}C	100
Total exchange capacity (Na-form), min	1.95 mmol Cu/g
Expected operating capacity (Na-form)	1.49 mmol Cu/g

* The values are copied from the technical data sheets provided by the manufacturers and are available online: http://www.suqing.com/Engpage/production/Cation3.htm

ACCEPTED MANUSCRIPT

2.1.2 Pre-treatment of Resins

The pretreatment of the resins was to ensure a consistent resin condition for all the experiments. Therefore, fixed amounts of HCl and NaOH were used and the same pretreatment steps were used to condition the resins throughout the study.

The resin was treated with the standard regeneration procedure and to pre-treat the resins to ensure a uniform standard condition. The resin sample was first immersed in 8% HCl (the amount of HCl would be based on a dosage of 180g HCl per liter wet resin) for 45 minutes with stirring. The resin was then rinsed with deionized water to remove the residual of HCl. After that, the resin was immersed in 4% NaOH for another 45 minutes. The Na concentration in the acid solution was measured using ICP-AES so that the Na content in the resin could be calculated. The 100% sodium form of resin changed the solution pH highly alkaline and precipitated nickel hydroxide causing the column to block.

Consequently a hydrogen-sodium resin was used and to condition the resin to this form (the actual resin Na-content was later measured to be 3.06meq/g), a dosage of 41.2g NaOH per liter wet resin was used. The resin was first prepared in the hydrogen form and then a titration experiment of the resin was carried out with different amounts of NaOH. From the titration experiments, a Na+ content of 3.06 meq/g could be achieved based on the addition of the 41.2g of NaOH. The pretreatment was designed to produce this resin in hydrogen-sodium form with Na content of 3.06 meq/g Na^+ and by difference a H+ content of 1.64meq/g resin .

Finally, the resin was rinsed with deionized water until the pH is about 11.5 to remove residual NaOH. After that, the resins were dried in an oven using a

ACCEPTED MANUSCRIPT

temperature below or equal to 110°C for more than 48 hours. Finally, the resins were cooled in desiccators and sieved to within the particle size range of 1000-450 μm after cooling.

2.1.3 Nickel Ion Solution

Nickel(II) chloride ($NiCl_2 \cdot 2H_2O$) (99%) was supplied by Riedel–de-Haën Chemicals. Stock metal solutions were prepared by ultra-pure deionized water. Metal ion solutions of varied concentrations were made up by diluting the stock solution with different amounts of deionized water.

2.2 Experimental Procedures

2.2.1 To measure the Equilibrium Isotherms

In order to investigate the pH effect on the ion exchange capacity, 0.1g resin (with 3.06meq/g Na content and 1.64meq/g H content) was added to sample bottles containing 50ml nickel chloride of various concentrations from 0.5 to 6.0mmol/dm^3. The sample bottles were then agitated at 200rpm at a constant temperature of 25+/-2 degC for 72 hours to achieve equilibrium. The nickel ion solution concentrations were measured using ICP-AES.

- The final pH of each test bottle was also measured.
- The amount of metal ion sorbed, q_e, was calculated using the following equation:

$$q_e = \frac{(C_o - C_e)V}{m} \qquad (1)$$

- Finally, the exchange capacity, q_e, was plotted against the equilibrium pH.

2.2.2 To Study the Effect of Equilibrium pH on Ion Exchange Capacity

In order to investigate if the exchange capacity varied with the solution pH a series of studies was performed using similar conditions to those described in section 2.2.1,

ACCEPTED MANUSCRIPT

but with a fixed initial concentration on nickel chloride at 6.0mmol/dm^3 and with different initial solution pH values.

2.3 Fixed Bed Column Studies

2.3.1 Fixed Bed Experimental Setup

A pilot-scale ion exchange system was built to conduct the column runs. The schematic diagram of the setup is shown in Figure 2.

The ion exchange columns were made of Perspex tubes with an internal diameter of 2.08cm and a height of 150cm. It was assumed that there was no variation of the axial liquid velocity and solute concentration in the radial direction inside the column. The column diameter to the particle diameter ratio for this experiment ranged between 21 and 46, which was considered to be adequate such that the effects of channeling at the wall and random variations in the interstitial velocity within the bed became negligible. The top and bottom of the column were connected to 0.5 cm Perspex tubes which were the inlet and outlet of the column respectively. A retaining sieve of 65 mesh size was fixed at the bottom of the column using a special adhesive. Ballotini balls of 2mm diameter were placed at the column bottom before putting in the resin. 5 samples points were located at 0cm, 20cm, 40cm, 60cm and 80cm from the column bottom along the straight height of the column. Each point was sealed using Suba-seals and 5 syringes of 5cm^3 were used to collect samples from these sampling points for analysis.

The metal ion solutions were prepared by dissolving a specific amount of metal ion salt in deionized water in the mixing tank where the metal ion solution was continuously circulated by a centrifugal pump. The pH of the metal solutions would also be adjusted slightly by adding HCl or NaOH to maintain a constant pH of about

ACCEPTED MANUSCRIPT

5.0. According to the speciation diagrams for Ni, under the pH of 5.0, the predominant species is Ni^{2+} [29].

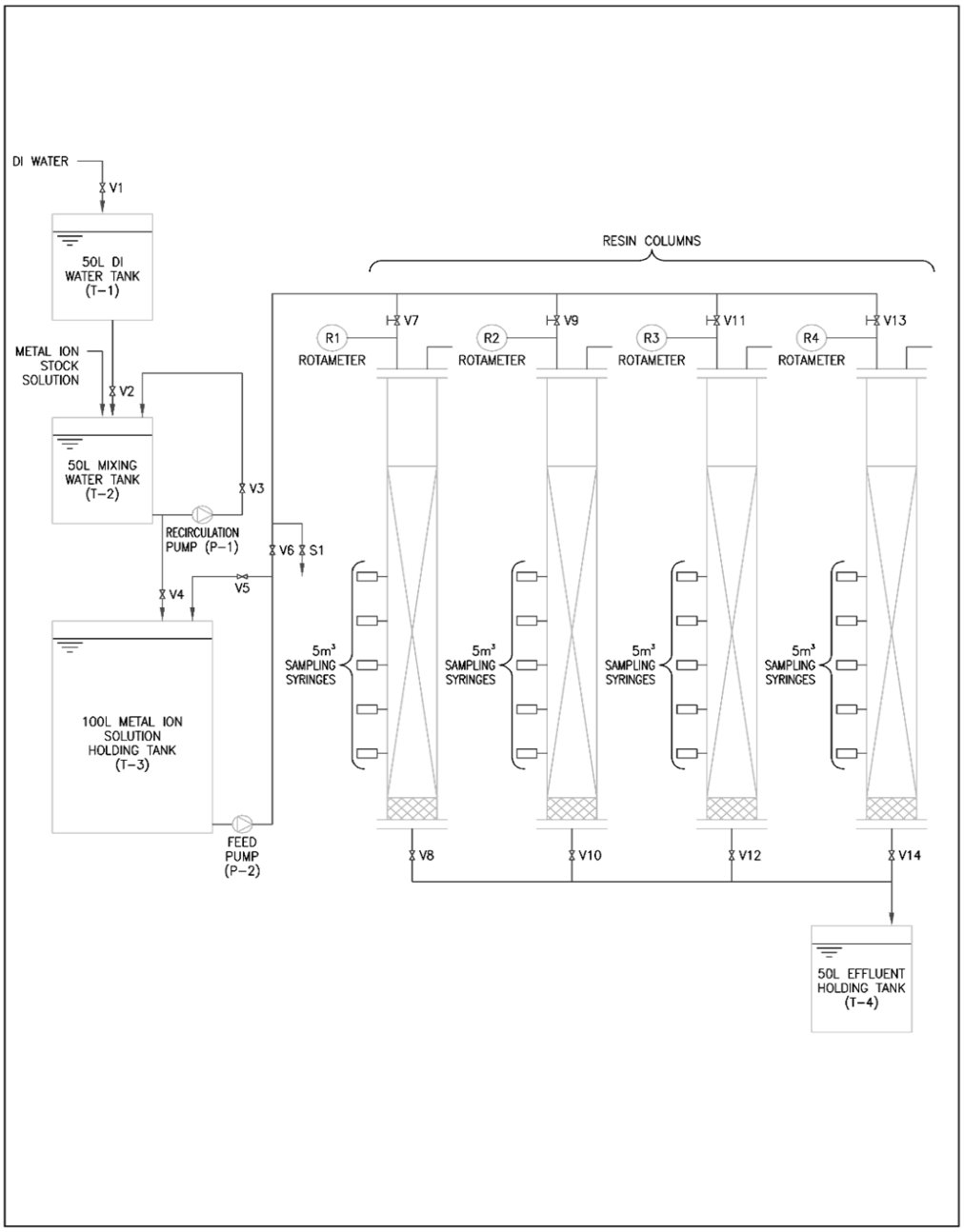

Figure 2. Schematic diagram of the experimental setup

ACCEPTED MANUSCRIPT

The single component metal ion solution was delivered to the holding tank where the metal ion solution was pumped to each column via a rotameter. The rotameters were used to monitor the flowrate which would be maintained constant throughout the experiment. The flowrates used in the column runs were in the range of 120-220 ml/min. The linear velocity was in the range of 0.66-1.04 m/s. Depending on the flow rate and the resin bed depth, the empty bed residence time (EBRT) varied from about 40s to 200s.

2.3.2 Fixed Bed Experimental Procedures

A specific amount of pretreated dry resin (i.e. 145g) would be packed into each column. Before packing, the dry resin was first soaked in deionized water for 24 hours so that all the air could be expelled from the resin. Then the wet resin, together with the deionized water, was poured into the columns. During the column filling procedure, the resin should be kept submerged in deionized water. It was important to ensure that all air was expelled from the resin bed. If air pockets existed in the packed column, the operation would become unstable as channeling and air locking would occur. After packing the column, the column was tapped well so as to allow the resin to settle down. After filling in the resin, the column would be covered by the top flange.

To start the experiment, the metal ion solution in the holding tank would be pumped at constant flowrate to the ion exchange columns. Samples were taken along the column at time intervals ranging from 30 minutes to half an hour until the metal ion concentration of the effluent coming out from the column bottom reached the breakthrough point.

ACCEPTED MANUSCRIPT

2.4 Analytical Techniques

The concentrations of metal and sodium ion solutions were measured by Inductively Coupled Plasma-Atomic Emission Spectrophotometer (ICP-AES). Three calibration standards and blank solution were used to form four points to establish the calibration curve for the equipment. The calibration standards were prepared using the standard solutions which were certified by the supplier. A linear calibration line was obtained after the calibration procedure. If the correlation coefficient R^2 was less than 0.999, the machine would be re-calibrated to ensure the accuracy of results. The samples were automatically measured three times in one aspiration. If the standard deviation of test results was greater than one percent, the samples were measured again until the test results fulfilled the analysis requirement.

3.0 Model Development

Several simplified design models based on general assumptions and lumped mass-transfer parameters are available, such as, the bed depth service time (BDST) model and the empty bed residence time (EBRT) model. Apart from these, several models based on fundamental mass transport mechanisms, including the homogeneous surface diffusion and shrinking core pore diffusion models, have been investigated and modified to identify the most appropriate model to describe the fixed bed removal of heavy metals ions by the chelating resin. The major drawback for these mass transfer models is that they require accurate correlations for mass-transfer parameters to describe external film, internal pore diffusion and the equilibrium relationship between resin and metal ions, and also need the solution of a number of differential equations. However, by using these mathematical models, the extent of pilot-plant testing could be reduced and used mainly for verification rather than

ACCEPTED MANUSCRIPT

information gathering, which can save a lot of time in designing the ion exchange systems.

3.1 Development of Homogeneous Surface Diffusion Model (HSDM)

The HSDM is one of the most widely used dual-resistance diffusion models evolved from the efforts to simulate and predict fixed bed adsorption processes. This model supposes that adsorption occurs on the outer surface of the adsorbent, followed by the diffusion of the adsorbed phase into the particles.

This model was first developed by Rosen [30,31] who considered the resistances of both liquid film and solid diffusion into spherical particles and presented an analytical solution for this model for fixed-bed systems with a simple, linear equilibrium relationship. Several modifications, improvements and limiting assumptions have been developed since this approach. The detailed literature review covering the developments up to recent years is included in the Supplementary information. More recent developments and applications of the HSDM include the design of GAC filters for a full scale groundwater facility [32], a solution to HSDM using orthogonal collocation [33] and a review and comparison of the different solution methods of the various HSD models [34].

The algorithm of our model is shown in Figure 3. A computational program based on the above mathematical model has been developed in Fortran 77.

ACCEPTED MANUSCRIPT

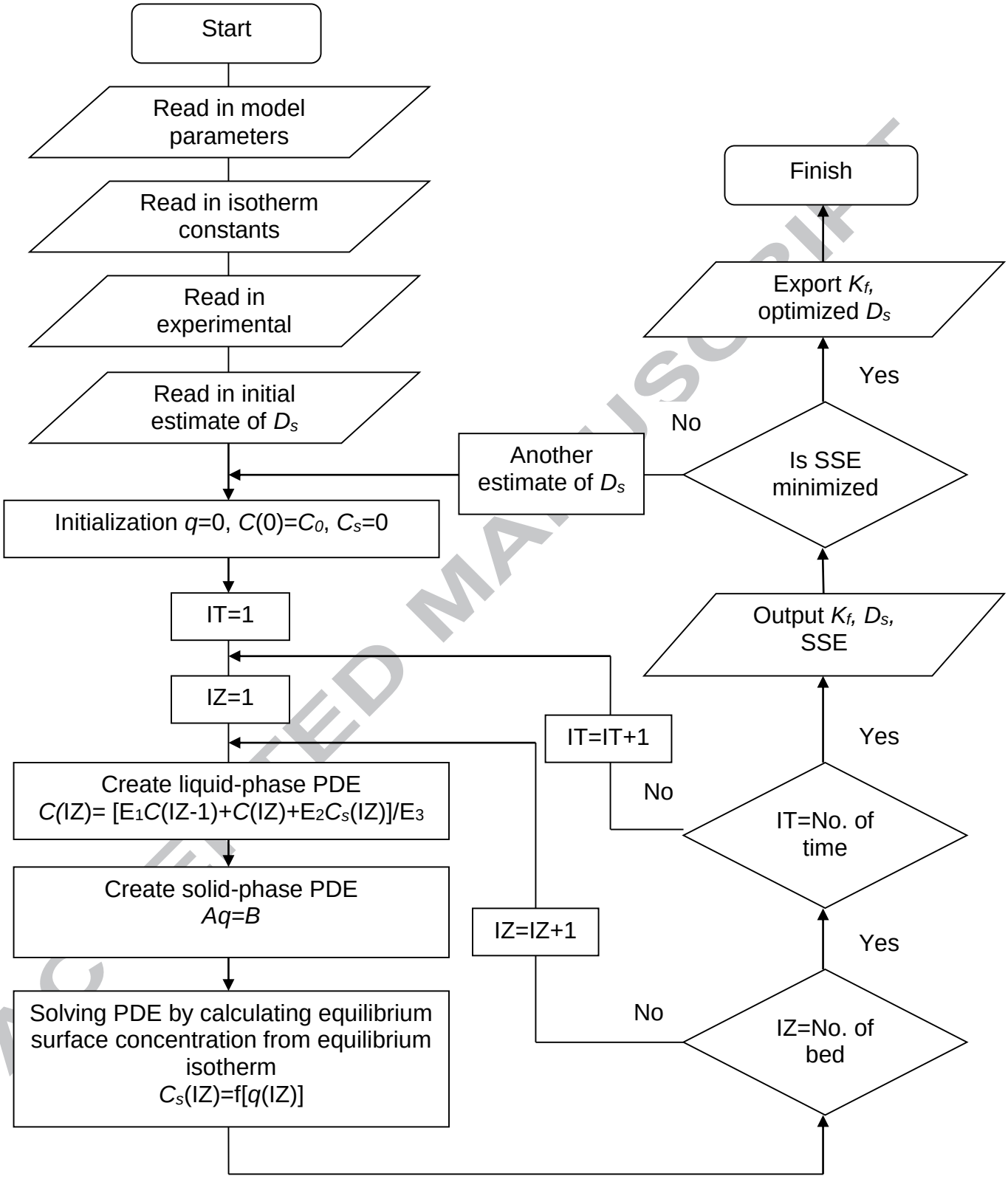

Figure 3 Algorithm for Homogeneous Surface Diffusion Model

ACCEPTED MANUSCRIPT

Model parameters, such as external mass transfer coefficient and surface diffusivity, can be optimized in the program in order to obtain the best fit curve to the experimental data. The optimization method employed in the model program is the downhill simplex method from Nelder and Mead [35]. This is done by performing a multidimensional minimization of the objective function, i.e. the SSE between the experimental data and the model prediction. The full set of equations and the development of the model are presented in the Supplementary Information section.

4.0 Results and Discussion

4.1 Equilibrium Isotherms

The metal adsorption process of the iminodiacetate chelating resin is actually an equilibrium system comprising Na^+, H^+ and metal ions. Hydrolysis and protonation will take place as well during the metal ion exchange process. Thus, the solution pH will shift when the metal ions are exchanged by the resin. When the solution pH shifts up too much, metal hydroxide precipitation will occur, whereas, if the solution pH shifts downwards then competitive protonation with hydrogen ions becomes obvious and the metal ion uptake capacity will decrease. Both metal precipitation and protonation can interfere with the determination of the resin's true ion exchange capacity, and in turn distort the equilibrium isotherms. In this regard, when batch tests are used to determine equilibrium isotherms, special care should be taken to make sure that the equilibrium isotherms are not distorted by the pH shift.

ACCEPTED MANUSCRIPT

ACCEPTED MANUSCRIPT

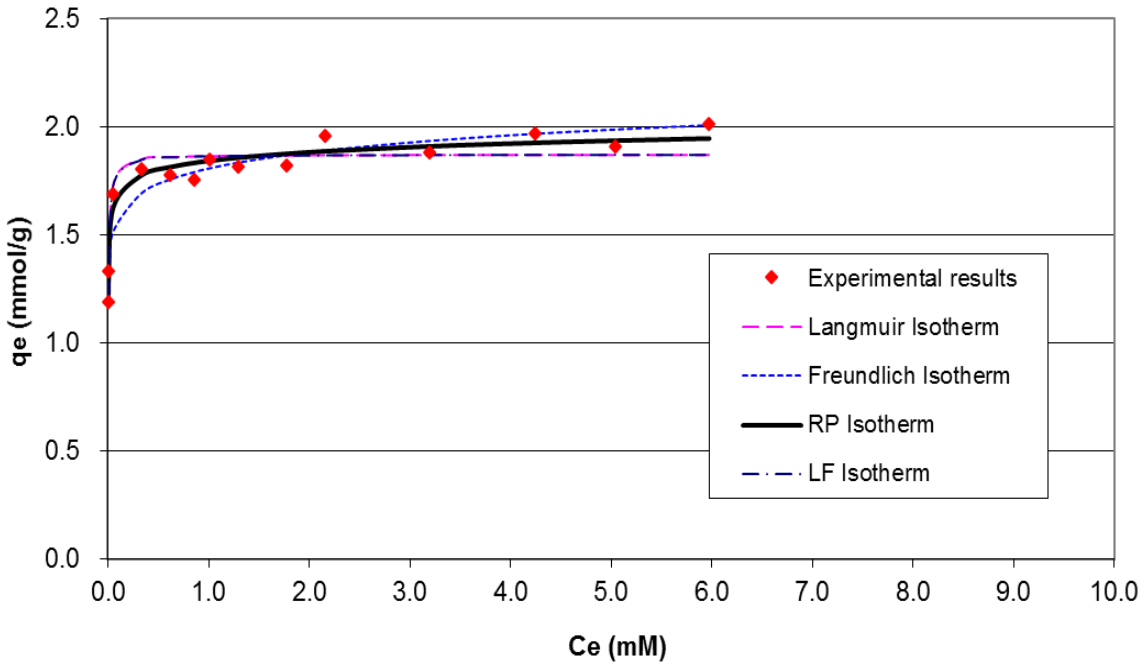

Figure 4. Experimental and theoretical model isotherms.

The experimental equilibrium points are shown in Figure 4. The data were analysed using four isotherm models, namely, the Langmuir, Freundlich, Langmuir-Freundlich (Sips) and the Redlich-Peterson isotherms. The optimum values of the isotherm equation constants were determined by the SSE error analysis using MS Solver. The best fit curves for each of the four models are shown in Figure 4. The lowest SSE was obtained for the Redlich-Peterson isotherm.

4.2 Effect of Equilibrium pH on Ion Exchange Capacity

4.2.1 Titration of Resin and Sodium Uptake

In order to optimize the nickel exchange capacity in the columns while preventing precipitation and protonation, the resin was titrated with NaOH. Using the hydrogen form of resin as the reference the composition of three basic forms of the resin, i.e. hydrogen form (0 meq/g Na^+), hydrogen-sodium form (3.06 meq/g Na^+) were measured from the resins used in the column

ACCEPTED MANUSCRIPT

runs) and the sodium form (4.43 meq/g Na^+) as the theoretical maximum value calculated from the mass balance), is determined and shown in Table 2. From the projection, the hydrogen-sodium form resin used in the column runs is found to have 5.49 meq/g exchange sites but only 4.70 meq/g sites are easily available for ion exchange, which are loaded with 3.06 meq/g Na^+ ions and 1.64 meq/g H^+ ions. Thus, the resin used in these studies can be viewed as the one containing a mixture of Na-loaded and H-loaded exchange sites.

Table 2. Expected composition of resins with different sodium contents

Resin Na content (meq/g)	Estimated exchange site (meq/g)	Correction factor	Active exchange sites (meq/g)	Expected Na-loaded sites (meq/g)	Expected H-loaded sites (meq/g)
0	6.32	1.00	5.40	0	5.40
3.06	5.49	1.15	4.70	3.06	1.64
4.43	5.18	1.22	4.43	4.43	0

Any ion exchange process of this hydrogen-sodium form resin is actually an exchange process with both of the Na^+ and H^+ ions in the resin as pointed out by Lehto *et al.* [36] and Leinonen *et al.* [24]. This resin composition was used in the column studies.

Based on Table 2 the fully saturated capacity of the resin for the divalent nickel ion is based on 3.06meq (from Na^+ exchange) + 1.64meq (from H^+ exchange) providing the fixed bed adsorption columns are operated to ensure the effluent pH is maintained above 4.5 and below 7.0. This will result in a theoretical maximum nickel uptake of 2.35meq Ni/g resin.

4.2.2 Mass Balancing

In order to assess the operating performance of the ion exchange resin relative to the theoretical data estimated in Table 2, a mass balance was carried out on the pilot column experimental data shown in Figure 4 for the highest flowrate of 220 ml/minute. Since the Na+ exchange process is

ACCEPTED MANUSCRIPT

very much faster than the H+ process the changeover in mechanism can readily be observed at $C_t/C_0 = 0.70$ and a time of 580 minutes.

The metal exchange capacity for each resin exchange ion can be calculated by evaluating the area bounded by the experimental points in Figure 5, for the sodium ion exchange and then for the hydrogen ion exchange zone; using the following relationship:

M^+ Exchange = 2 [C_0 x t (Operating Time) x $F^/$ x C_F (Capacity Factor)]/M_R (Resin Mass)

Where C_0 = initial Ni^{2+} concentration (mM/dm^3)

t = operating time (minutes)

$F^/$ = solution flowrate (dm^3/minute)

C_F = bed capacity factor (fraction of bed saturated eg for Na, then $C_F = 1.0$)

M_R = resin mass

For Na^+ exchange:

= 2[1.7 mM/dm^3 x (580-0) min x 0.22 dm^3/min x 1.0]/145g = 2.992 mM Na^+

For H^+ exchange:

= 2[1.7 mM/dm^3 x (2200 - 580) min x 0.22 dm^3/min x 0.15]/145g = 1.254 mM H^+

In this case the capacity factor from Figure 5, represents the mean breakthrough between the time increment 2200 minutes and 580 minutes, or, (1.00 - 0.70)/2 = 0.15. Based on the total available ions in Table 2 the sodium capacity is 97.8% of saturation and the hydrogen capacity is 76.5% of the saturation capacity for sodium.

ACCEPTED MANUSCRIPT

4.3 Fixed Bed Mass Transfer Modeling

In the present study, the homogeneous surface diffusion model has been used to correlate the experimental data of the fixed-bed chelating ion exchanger. The model is a dual-resistance model based on the assumption that external film diffusion and intraparticle diffusion (pore or surface or pore and surface diffusion) are the two most likely rate-controlling mechanisms in the ion exchange process. The factors influencing external mass transfer coefficients will be discussed. The model has been described in section 3 and the mathematical development is presented in the supplementary materials.

4.3.1 Determination of Model Parameters

External Film Diffusion Coefficient

The external film diffusion coefficient, k_f, for the fixed bed systems can be determined by empirically correlating with the dimensionless Sherwood number, *Sh*, which is a function of the Reynold number, *Re*, and Schmidt number, *Sc*, as shown in equation (2).

$$Sh = \frac{k_f d_p}{D_{mol}} \tag{2}$$

where the bulk liquid diffusivity, D_{mol}, for Ni^{2+} is 7.14×10^{-6} cm^2/s based on the literature [37].

$$Sh = f(Re, Sc) \tag{3}$$

where

$$\mathrm{Re} = \frac{\rho v d_p}{\mu} \tag{4}$$

ACCEPTED MANUSCRIPT

$$\mathrm{Sc} = \frac{\mu}{\rho\ D_{mol}} \qquad (5)$$

For mass transfer in both laminar and turbulent flow, Eq. (6) is commonly in the form of:

$$Sh = A + B \times \mathrm{Re}^{\varphi 1} \times Sc^{\varphi 2} \qquad (6)$$

where A, B, φ_1, φ_2 are empirical constants obtained by fitting the experimental data.

A number of empirical correlations based on the above general form of Eq. (6) have been derived by the previous researchers. Each of these empirical correlations is applicable for a certain hydrodynamic regime which is usually represented by *Re*. Due to different packing densities of the resin columns, the actual bed void fraction, ε, may vary slightly among the column experiments. The values of bed void fraction, ε, Reynolds number, *Re* and ε *Re* for all the column experiments in the present study are summarized in Table 3.

Table 3 Values of *Re* and ε *Re* for all the column experiments

Metal Ion	Flowrate (ml/min)	C_o (mM)	Mean d_p (μm)	Void Fraction ε	*Re*	ε*Re*
Ni	120	1.7	725	0.36	15.5	5.6
Ni	140	1.7	725	0.37	17.8	6.5
Ni	180	1.7	725	0.38	22.1	8.4
Ni	220	1.7	725	0.38	26.8	10.2
Ni	180	1.0	725	0.38	22.2	8.4
Ni	180	2.1	725	0.37	22.4	8.4

In view of the hydrodynamic conditions of the column experiments, the following three empirical correlations are found to be most applicable to this present study.

ACCEPTED MANUSCRIPT

Williamson *et al*. [38] proposed the following correlation of Sherwood number for liquids under the conditions of 0.08 < *Re* < 125 and 150 < *Sc* < 1,300:

$$Sh = 2.4\varepsilon Re^{0.34} Sc^{0.42} \quad (7)$$

Wilson and Geankoplis [39] used methods similar to those of Williamson *et al*. but under slightly different conditions and extended the applicable range down to *Re* = 1.6 x 10^{-3}. They modified Eq. (7) to:

$$Sh = \frac{1.09}{\varepsilon} \mathrm{Re}^{1/3} Sc^{1/3} \quad (8)$$

Eq. (8) is recommended for the range of 0.0016 < *Re* < 55.

Roberts *et al.* [40] proposed a simplified Gnielinski's correlation:

$$Sh = (2 + 0.644 Re^{1/2} Sc^{1/3})[1 + 1.5(1 - \varepsilon)] \quad (9)$$

The recommended applicable range of Eq. (9) is 3 < ε *Re* < 1,000.

As an example to compare the three correlations, the values of k_f for the Ni ion exchange system (with conditions of C_o=1.7mM, flowrate=220ml/min and mean d_p=725 μ m) calculated from the three empirical correlations are listed in Table 4. As shown in the table, the values of k_f derived from the three correlations are actually quite close to each other, which is considered to have little influence to the model prediction on fixed-bed breakthrough behavior as reflected from the SSE and the sensitivity analysis for the HSD model.

In spite of this, as the simplified Gnielinski's correlation generally gives the smallest SSE in the modeling simulations among the three k_f correlations, the simplified Gnielinski's correlation will be used to calculate the external diffusion coefficient, k_f, in the present study.

ACCEPTED MANUSCRIPT

Table 4 **Values of k_f for Ni ion exchange system, (C_o=1.7mM, flowrate=220ml/min, mean d_p=725 μm)**

Empirical correlations	k_f (x10^{-3}cm/s)	SSE		
		HSDM	SCDM (x10^6)	Modified SCDM
Williamson *et al*. [38]	4.22	0.64	0.86	0.43
Wilson and Geankoplis [39]	6.83	0.77	0.86	0.52
Simplified Gnielinski's correlation [40]	5.41	0.69	0.86	0.37

4.3.2 Intraparticle Diffusion Coefficient

Depending on which diffusion model we are using, the intraparticle diffusion coefficient can be the surface diffusivity D_s for the homogeneous surface diffusion model or the effective pore diffusivity D_{eff} for the shrinking core pore diffusion model. Optimum values of the intraparticle diffusion coefficient will be determined during model calibration, i.e. fitting the modeled curves with the experimental data, in which an optimization routine involving minimization of the sum of the errors between the calculated and experimental data points will be used.

4.3.3 Other Model Parameters

Apart from the diffusion coefficients, appropriate values of the other model parameters, like the equilibrium isotherm constants for the homogeneous surface diffusion model or the hypothetical bed capacity, q_e^h for the Redlich-Peterson equilibrium model, will also be determined when doing the modeling.

4.4. Homogeneous Surface Diffusion Model (HSDM)

The basic model parameters governing the HSDM include the surface diffusivity D_s inside the resin particle, and the external mass transfer coefficient across the liquid boundary layer outside

ACCEPTED MANUSCRIPT

the resin surface, k_f and the constants of the Redlich-Peterson equilibrium isotherm. While the RP isotherm parameters were determined from the experiments and the k_f value was calculated from the simplified Gnielinski's correlation, Eq. (9), a FORTRAN program was used to optimize the D_s value so as to obtain the best fit curves to the experimental data.

4.4.1 Sensitivity Analysis

Sensitivity analysis was performed to observe the effects of varying the model parameters on the simulation. The Ni ion exchange system with conditions of C_o=1.7mM, flowrate=220ml/min and mean d_p=725 μm was taken as a sample for the sensitivity analysis. The Na^+/Ni^{2+} exchange is designated Part 1 and the $H^{+/}Ni^{2+}$ is designated as Part 2.

Table 5 HSDM parameters for the Ni ion exchange system (C_o=1.7mM, flowrate =220ml/min, mean d_p=725 μm)

	Part 1	Part 2
D_s (x10^{-7}cm^2/s)	224	0.0036
k_f (x10^{-3}cm/s)	5.41	5.41
K_{RP}	351	781
a_{RP}	423	423
b_{RP}	0.97	0.97
q_{max} (mmol/g)	0.696	1.512

A single set of values for the model parameters cannot fit the whole length of the breakthrough curve. Instead, two sets of optimum values are needed to best simulate the breakthrough curve because there is a sharp change in the slope of the curve. The model parameters used in the sensitivity analysis are shown in Table 4 and the model outputs in Figures 5 and 6..

As illustrated in Figure 5, a very high value of surface diffusivity, *Ds* is required in order to model the sharp rise in the first part of the breakthrough curve. The optimum value of *Ds* is

ACCEPTED MANUSCRIPT

found to be $2.24x10^{-5}cm^2/s$ which is much higher than those identified in other previous studies using the HSDM. For instance, the *Ds* values for the adsorption of Cu, Cd and Zn on bone char were reported to be $2.46x10^{-9}cm^2/s$, $2.52x10^{-9}cm^2/s$ and $4.79x10^{-9}cm^2/s$ respectively by Ko *et al.* [41]. The difference may be attributed to the macroporous nature of the chelating resin used in this present study allowing the mass transfer rate to be controlled mostly by external film/.boundary layer diffusion. High *Ds* value implies that the intraparticle diffusion resistance in the first part of breakthrough is rather minimal and external boundary layer diffusion is important. Besides, the sensitivity analysis also reveals that the modeled curve changes only a little even though the *Ds* varies from $7x10^{-7}cm^2/s$ to $5x10^{-4}cm^2/s$. However, the modeling program would become unstable and cannot generate a numerical solution if the *Ds* value continues to reduce to less than $7x10^{-7}cm^2/s$. The reason for this is because a reduced *Ds* would lead to a higher surface diffusion resistance in the resin particle. Thus, a greater solid phase concentration gradient, which means a greater driving force, is needed to maintain the same diffusion rate. Since the solid phase concentration at the resin centre cannot be less than zero, it may become impossible for the equilibrium isotherm equation to couple the solid and liquid phase concentrations at the resin surface, if the *Ds* value falls beyond the applicable range.

ACCEPTED MANUSCRIPT

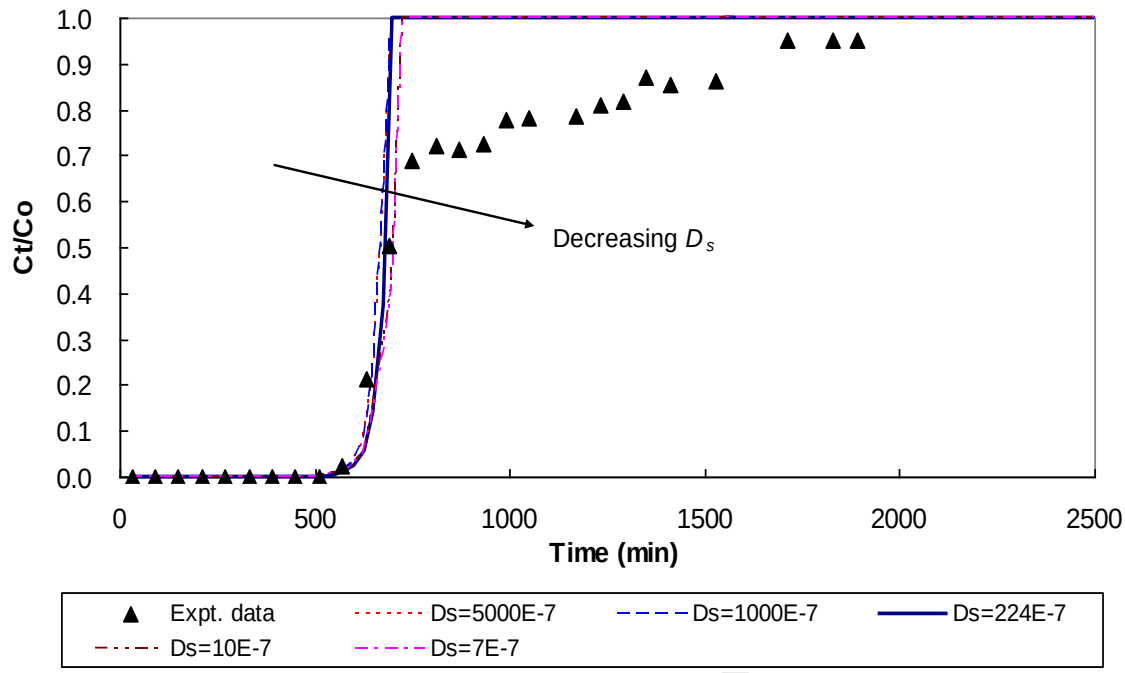

Figure 5. Sensitivity analysis of HSDM w.r.t. D_s for the first part of the breakthrough curve (Ni ion exchange, C_o=1.7mM, flowrate=220ml/min, mean d_p=725 μm)

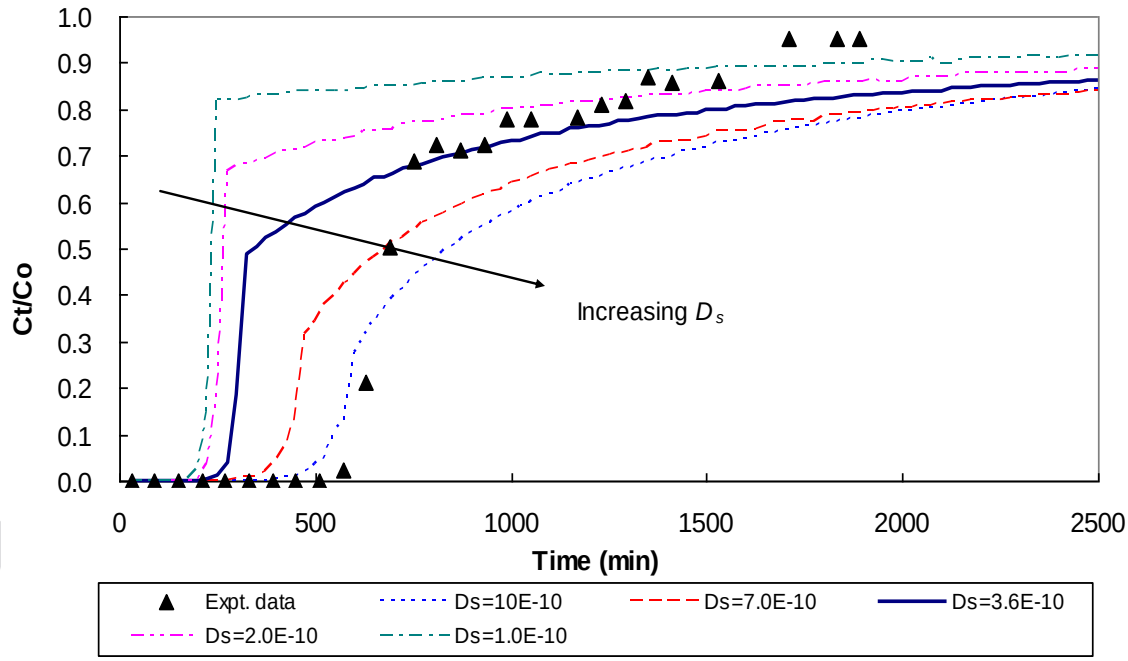

Figure 6. Sensitivity analysis of HSDM w.r.t. D_s for the second part of the breakthrough curve (Ni ion exchange, C_o=1.7mM, flowrate=220ml/min, mean d_p=725 μm)

ACCEPTED MANUSCRIPT

The insensitivity to this range of diffusion coefficient values for the $2Na^{+}$--Ni^{2+} exchange arises because the mass transfer, for this exchange, is controlled by the external boundary layer transfer coefficient, k_f, which is shown in Figure 7.

The optimum *Ds* value dramatically reduces to $3.6x10^{-10}cm^2/s$ in the second part of the breakthrough curve. This reflects the change of the ion exchange process from a fast one to a slow one as the process moves from sodium exchange to hydrogen exchange. As shown in Figure 6, with the new set of model parameters, the model prediction can only fit the second part of the breakthrough curve after the breakpoint. Since the *Ds* for the second part is rather small, even a very small change in the *Ds* value can already alter the shape of the modeled curve substantially.

Figure 7 and Figure 8 illustrate the effects of external film diffusion coefficient, k_f on the model prediction for the first and second parts of the breakthrough curve respectively. The k_f calculated from the simplified Gnielinski's correlation, Eq. (5), is $5.41\ x10^{-3}cm/s$. Assuming that the flow conditions around the resin particles would not change during the ion exchange process, the same value of k_f will thus be used for the first part and second part of the breakthrough curve.

As shown in Figure 7, the k_f calculated from the simplified Gnielinski's correlation gives a good fit to the experimental data for the first part of the breakthrough curve. Increasing the k_f value from the calculated value will mean reducing the film diffusion resistance and will therefore diminish its influence on the modeled curve. Whereas, decreasing the k_f value will deviate the modeled curve from the experimental data, especially for the initial part of the breakthrough curve. In the second part of the breakthrough curve, the surface diffusivity, *Ds*, is rather small so that the mass transfer is predominantly controlled by intraparticle diffusion.

ACCEPTED MANUSCRIPT

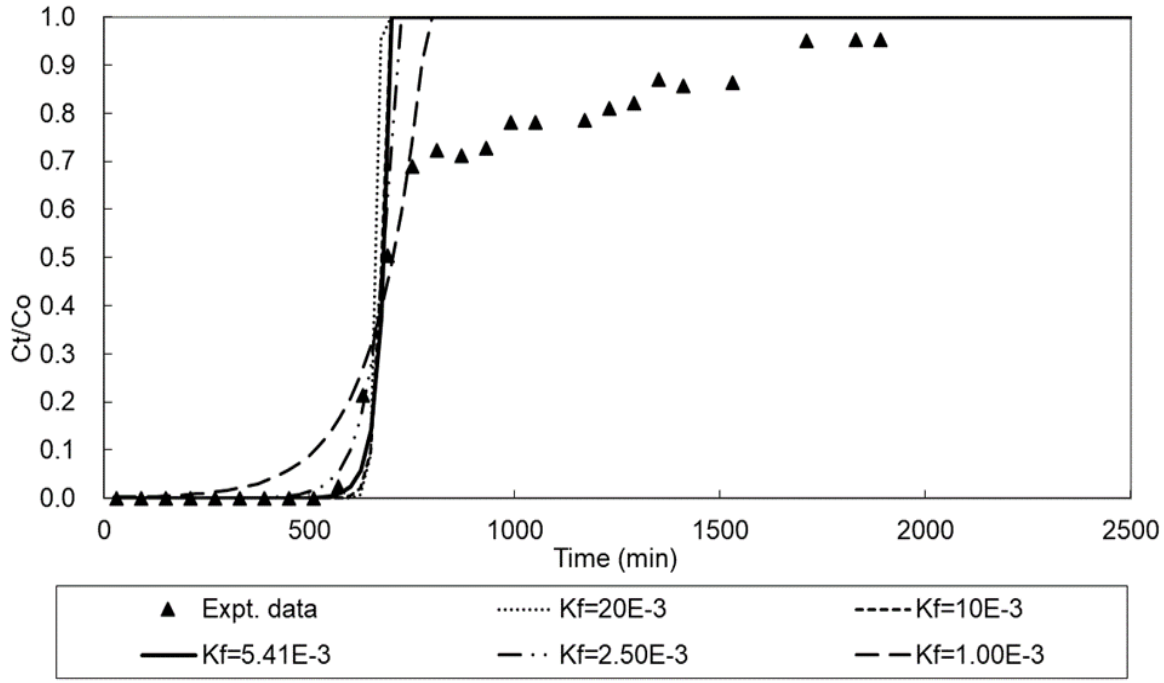

Figure 7. Sensitivity analysis of HSDM w.r.t. k_f for the first part of the breakthrough curve (Ni ion exchange, C_o=1.7mM, flowrate=220ml/min, mean d_p=725 μm)

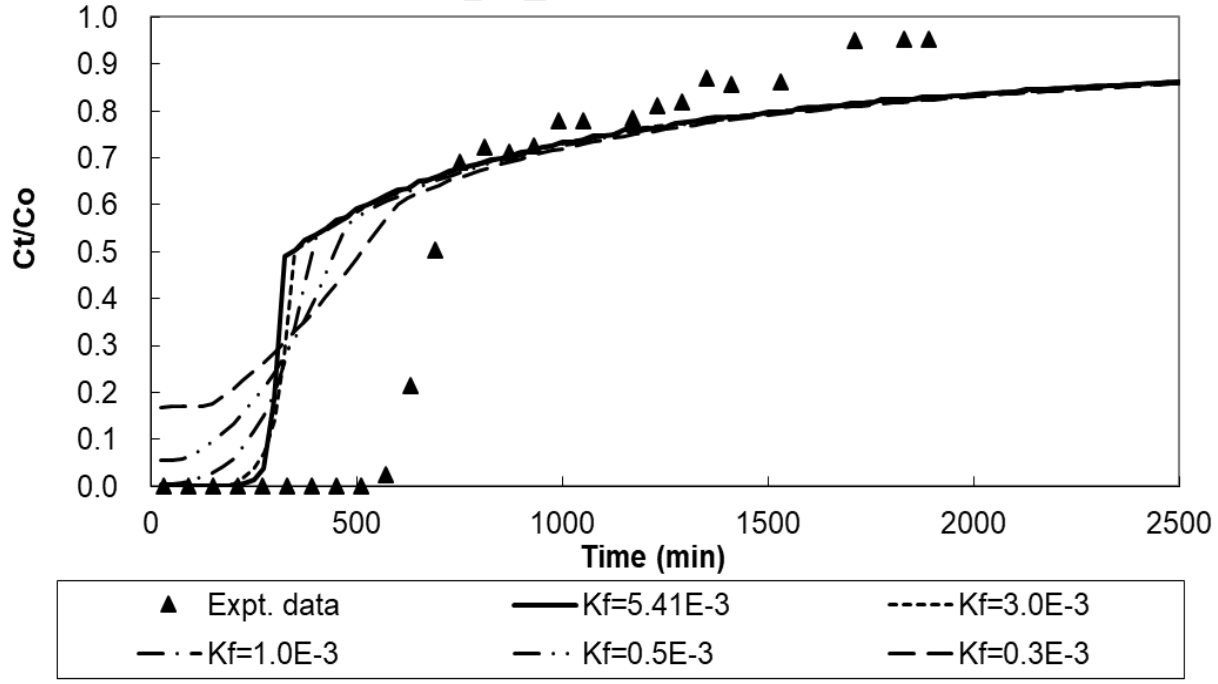

Figure 8. Sensitivity analysis of HSDM w.r.t. k_f for the second part of the breakthrough curve (Ni ion exchange, C_o=1.7mM, flowrate=220ml/min, d_p=725 μm)

ACCEPTED MANUSCRIPT

Therefore, as demonstrated in Figure 8, the shape of the modeled curve is relatively insensitive to the change of k_f in Part 2 of the exchange process, except for the beginning of the breakthrough. However, only the model prediction after the breakpoint of the breakthrough curve would be used to fit the second part of the breakthrough curve.

In the HSDM, an equilibrium isotherm equation is needed to couple the liquid and solid phase concentrations at the resin surface. In the present study, the Redlich-Peterson isotherm was found to best describe the equilibrium as shown in Figure 4. The isotherm constants of the RP isotherm for the ion exchange of Ni, K_{RP} , a_{RP} and b_{RP} are 658, 423 and 0.97 respectively.

$$q_e = K_{RP}C_e /[1 + a_{RP}C_e^{bR}] = 658C_e/[1 + 423C_e^{0.97}] \qquad (10a)$$

Nevertheless, it is found that with these values plus the mass transfer coefficients input into the model, the predicted breakthrough curve will shift to the right-hand side of the actual breakthrough curve as shown in Figure 9. This implies that the model has overestimated the resin capacity and projected a much longer breakthrough time than the experimental data. In order to fit the experimental data, the resin capacity has to be reduced and the only way is to adjust the equilibrium constants of the RP isotherm equation. In view of the RP isotherm equation, Eq. (10), K_{RP} shall be adjusted while a_{RP} and b_{RP} shall remain the same. In doing so, the resin capacity can be changed without altering the shape of the predicted curve. To this end, the optimum values of the RP isotherm constants, K_{RP}, a_{RP} and $b_{RP,}$ are found to be 342, 423 and 0.97 respectively. Based on these new values, the maximum equilibrium solid phase concentration at the resin surface, q_{max} will be reduced from the original value of 1.87 mmol/g to 0.82 mmol/g.

ACCEPTED MANUSCRIPT

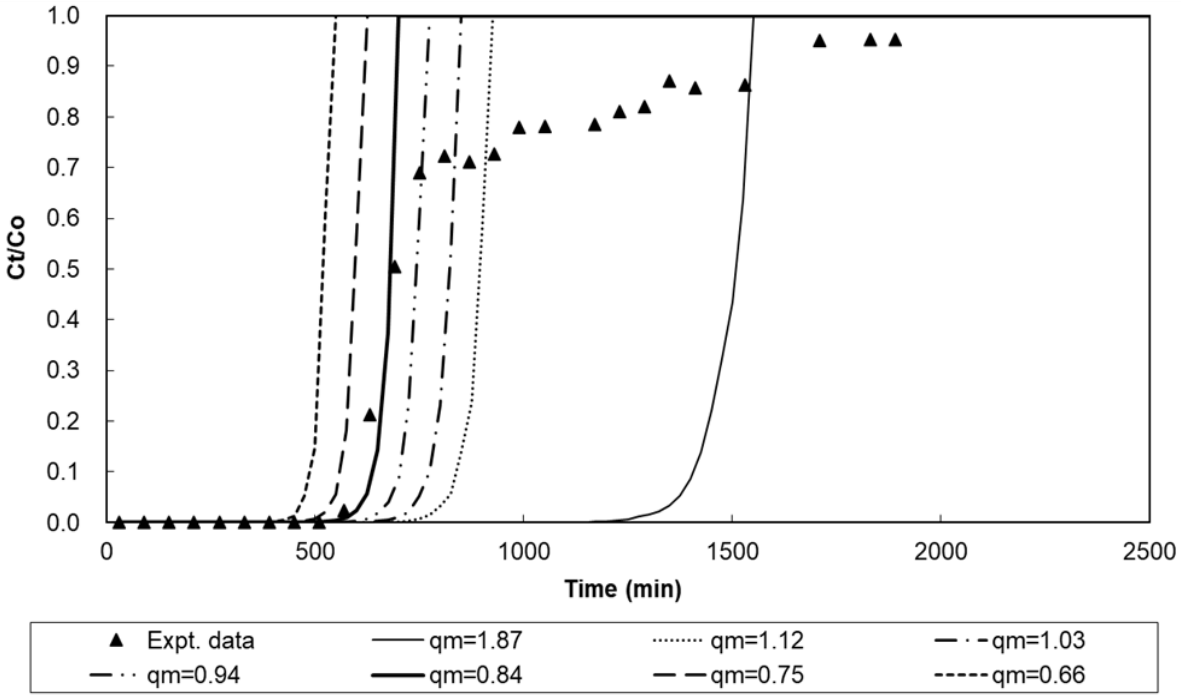

Figure 9. Sensitivity analysis of HSDM w.r.t. q_{max} for the first part of the breakthrough curve (Ni ion exchange, C_o=1.7mM, flowrate=220ml/min, mean d_p=725 μm)

Furthermore, the modified isotherm for the second part of the breakthrough curve is given by equation (10b):.

$$qe = K_{RP}C_e / [1 + a_{RP}C_e^{bR}] = 342C_e/[1 + 423C_e^{0.97}] \qquad (10b)$$

This time, when using the original values of the RP equilibrium isotherm constants, the model would underestimate the bed capacity and project a much shorter breakthrough time than the experimental data. The projected breakthrough curve will thus shift to the left-hand side of the actual breakthrough curve.

Now the HSDM model needs to be separated into, two components, the first part and second part of the breakthrough curve with two different sets of model parameters, $Ni^{2+}/2Na^{+}$ and $Ni^{2+}/2H^{+}$, using the second phase RP isotherm in order to give a realistic estimation of the resin capacity as shown in Figure 10..

ACCEPTED MANUSCRIPT

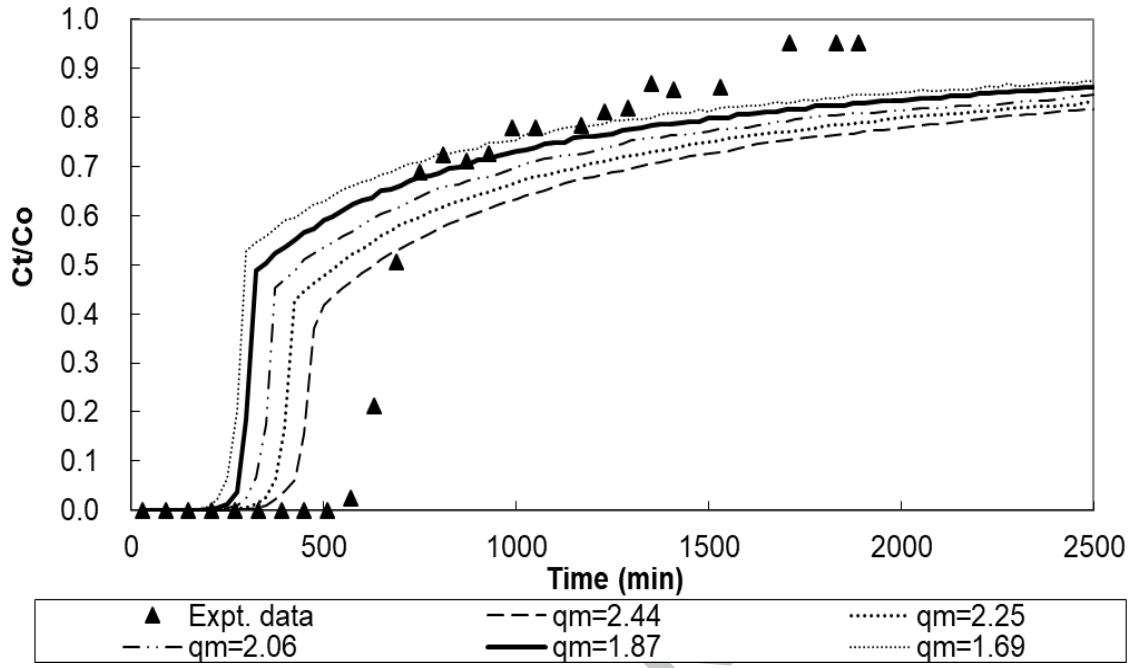

Figure 10. Sensitivity analysis of HSDM w.r.t. q_{max} for the second part of the breakthrough curve (Ni ion exchange, C_o=1.7mM, flowrate=220ml/min, mean d_p=725 μm)

The initial single cation (Na^+ or H^+) model assumes the ion exchange process to occur homogeneously throughout the whole resin, it is now necessary to model the first part and second part of the breakthrough process separately using the Redlich-Peterson equation for the capacity factor for each ion exchange, Ni → $2Na^{2+}$ and Ni → $2H^+$, and then combine the two model simulations to predict the overall breakthrough process.

The composite plot of the two ion exchange components is shown in Figure 10. We can observe the main mechanism changeover point at around Ct/Co = 0.7 in the figure. The model agreement in Part 1 and Part 2 with experimental data is very good. Part 1 indicates the exchange between the sodium form of the ion exchanger and nickel ions as represented in equation (11):

$$R\text{-}N\ (CH_2COONa)_2 + Ni^{2+} \rightarrow R\text{-}N\ (CH_2COO)_2\ Ni + 2Na^+ \qquad (11)$$

The external mass transfer coefficient, k_f = 5,41 x 10^{-3} cms^{-1}, and the surface diffusivity is 2.24 x

ACCEPTED MANUSCRIPT

10^{-5} cm^2s^{-1}. However, the diffusion coefficient is not sensitive over a wide range from Ds = 5 x 10^{-3} to 7 x 10^{-7} cm^2s^{-1}. Therefore, in Part 1 of the breakthrough layer, the rate controlling step is across the particle boundary layer and therefore the ion exchange reaction at the surface between $2Na^+$ and Ni^{2+} is very fast. A vertical breakthrough curve also indicates this mechanism.

Part 2 of the curve indicates the exchange between the hydrogen form of the ion exchanger and the nickel ions as shown in equation (12).

$$R\text{-}N\ (CH_2COOH)_2 + Ni^{2+} \rightarrow R\text{-}N\ (CH_2COO)_2\ Ni + 2H^+ \qquad (12)$$

In Part 2 of the breakthrough curve, Figure 6 and Figure 8 show the opposite trend to Part 1. There is little sensitivity to k_f after C_t/C_o = 0.7. However, the $2H^+$ exchange curve with Ni^{2+} was very sensitive to the surface diffusion coefficient, indicating that the mechanism in this section was surface diffusion controlled. Equation (12) indicates that the solution pH begins to fall due to the release of H+ ions and this controls the pH in the range 4.5 to 5.5; this prevents precipitation of nickel hydroxide and subsequent blockage of the column.

These resins are stable and leaching does not occur. Each iminodiacetate functional group contains one nitrogen atom and two oxygen atoms as the donor atoms that can form coordinate bonds with the heavy metal ion which is thus strongly bound to the resin. As shown from the breakthrough curve, basically complete sorption of heavy metal ions from the wastewater by the chelating resin until the resin is saturated and starts breakthrough. The desorption of heavy metal ions from the resin will only occur if the resin is regenerated by acid. The service life of the chelating resin is in general about 3-5 years.

ACCEPTED MANUSCRIPT

5.0 Conclusion

An iminodiacetate exchange resin has been used for the removal of nickel ions from wastewater. Initially using the full sodium form of the resin the column discharge was very alkaline precipitating nickel hydroxide and blocking the column. Consequently, a composite loaded exchange resin was developed comprising the sodium and hydrogen forms to optimize nickel removal and prevent precipitation with a ratio 3.06Na content (meq/g) and 1.64H content (meq/g) . A homogeneous surface diffusion model, incorporating a HSDM diffusion coefficient and an external mass transfer for the two systems: the values are Ni-Na (D_S = 224 x $10^{-7}cm^2s^{-1}$; k_f = 5.41 x $10^{-3}cms^{-1}$) and Ni-H (D_S = 3.60 x $10^{-10}cm^2s^{-1}$; k_f = 5.41 x $10^{-3}cms^{-1}$) respectively, was developed to predict the nickel breakthrough curve based on this binary ion exchange material and this model gave very good agreement between the theoretical breakthrough curve and the experimental breakthrough curve.

The key model parameters, such as external mass transfer coefficient and surface diffusivity, were optimized in the program in order to obtain the best fit curve to the experimental data. The optimization method employed in the model program is the downhill simplex method. This is done by performing a multidimensional minimization of the objective function, i.e. the SSE between the experimental data and the model prediction.

The actual column loading is 2.13meq Ni/g resin and the theoretical available capacity for this binary site resin is 2.35meq Ni/g resin, which represents 91% of the total available resin capacity. This model can be used for design purposes for single metal ion removal provided the resin site blend (Na:H) proportions are established experimentally to prevent precipitation and blockage in the column. However, for application to binary or multi- metal ion containing effluents more model development and testing are required.

ACCEPTED MANUSCRIPT

REFERENCES

[1] Y. Liu, J. Chen, Z. Cai, R. Chen, Q. Sun, M. Sun, Removal of copper and nickel from municipal sludge using an improved electrokinetic process, Chem. Eng. J. 307 (2017) 1008-1016.

[2] J. Sun, Q. Yang, D. Wang, S. Wang, F. Chen, Y. Zhong, K. Yi, F. Yao, C. Jiang, S. Li, X. Li, G. Zeng, Nickel toxicity to the performance and microbial community of enhanced biological phosphorus removal system, Chem. Eng. J. 313 (2017) 415-423.

[3] W.J.M. Dedietrich, F.P. Reinhard, Waste minimization and recovery technologies, Metal Finishing, 105 (10) (2007) 715-742.

[4] T.H. Eom, C.H. Lee, J.H. Kim, Development of an ion exchange system for plating wastewater treatment, Desalination, 180 (1-3) (2005) 163-172.

[5] G.D. Nielsen, U. Søderberg, P.J. Jørgensen, D.M. Templeton, P. Grandjean Absorption and retention of nickel from drinking water in relation to food intake and nickel sensitivity, Toxicology and Applied Pharmacology, 154(1) (1999) 67–75.

[6] M. Cempel, M., Nikel, G., Nickel: A Review of Its Sources and Environmental Toxicology, Pol. J. Environ. Stud., 15 (3) (2006) 375–382.

ACCEPTED MANUSCRIPT

ACCEPTED MANUSCRIPT

[7] K.A. Krishnan, K. G. Sreejalekshmi and R. S. Baiju, Nickel(II) adsorption onto biomass based activated carbon obtained from sugarcane bagasse pith, Bioresour. Technol. 102 (2011) 10239-10247.

[8] A. Warshawsky, Modern research in ion exchange, Ion Exchange: Science and Technology, NATO AISI Series, Rodrigues, A.E., Martinus Nijhoff Publishers, Boston (1986).

[9] M. Hudson, Coordination chemistry of selective ion exchange resins, Rodrigues, A.E., Ed.; in Ion Exchange: Science and Technology; NATO ASI, Series; Martinus Nijhoff Publishers: Boston, MA, 35-66 (1986).

[10] E. Eser, V.N. Tirtom, T. Aydemir, S. Becerik, A. Dinçer, Removal of nickel (II) ions by histidine modified chitosan beads, Chem. Eng. J. 210 (2012) 590-596.

[11] K.C.M. Kwok, V.K.C. Lee, G. McKay, Novel model development for sorption of arsenate on chitosan, Chem. Eng. J. 151 (1) (2009) 122-133.

[12] L.F. Koong, F.K. Lam, J. Barford, G. McKay, A comparative study on selective adsorption of metal ions using aminated adsorbents, J. Coll. Interf. Sci. 395 (2013) 230-240.

[13] A.K. Sengupta, Y. Zhu, D. Hauze, Metal (II) ion binding onto chelating exchangers with nitrogen donor atoms: some new observations and related implications, Environ. Sci. Technol. 25 (1991) 481-488.

ACCEPTED MANUSCRIPT

ACCEPTED MANUSCRIPT

[14] P. Hadi, J. Barford, G. McKay, Synergistic effect in the simultaneous removal of binary cobalt-nickel heavy metals from effluents by a novel e-waste-derived material, Chem. Eng. J. 228 (2013) 140-146.

[15] M.R. Moghbeli, A. Khajeh, M. Alikhan, Nanosilica reinforced ion-exchange polyHIPE type membrane for removal of nickel ions: Preparation, characterization and adsorption studies, Chem. Eng. J. 309 (2017) 552-562.

[16] A. Dabrowski, Z. Hubicki, P. Podkoscielny, E. Robens, Selective removal of the heavy metal ions from waters and industrial wastewaters by ion-exchange method, Chemosphere, 56 (2004) 91-106.

[17] A. Fernandez, M. Rendueles, M. Diaz, Equilibrium and activity coefficients in metal-iminodiacetic ion exchange, Afinidad, 53 (464) (1996) 235-254.

[18] E. Arevalo, A. Fernandez, M. Rendueles, M. Diaz, Equilibrium of metals with iminodiacetic resin in binary and ternary systems, Solvent Extr. Ion Exch. 17(2) (1999) 429–454.

[19] M. Pesavento, R. Biesuz, Characterization and application of chelating resins as chemical reagents for metal ions, based on the Gibbs-Donnan model, React. Funct. Poly. 36 (2) (1998) 135–147.

ACCEPTED MANUSCRIPT

ACCEPTED MANUSCRIPT

[20] E.M. Malla, M.B. Alvarez, D.A. Batistoni, Evaluation of sorption and desorption characteristics of cadmium, lead and zinc on Amberlite IRC-718 iminodiacetate chelating ion exchanger, Talanta, 57 (2002) 277-287.

[21] V.B. Kargman, L.P. Sokolova, G.K. Saldadze, G.S. Beklemisheva, A.K. Samsonov, Selective sorption recovery of metals from wastewater of electroplating productions, Russian J. Applied Chem. 74 (11) (2001) 1858 – 1863.

[22] R. Koivula, J. Lehto, P. Leena, T. Gale, H. Leinonen, Purification of metal plating rinse waters with chelating ion exchangers, Hydrometallurgy, 56 (2000) 93-108.

[23] F. Mijangos, M. Diaz, Metal-proton equilibrium relations in a chelating iminodiacetic resin, Ind. Eng. Chem. Res. 31 (11) (1992) 2524–2532.

[24] H. Leinonen, J. Lehto, Ion exchange of nickel by iminodiacetic acid chelating resin Chelex 100, Reac. Funct. Poly. 43 (2000) 1-6.

[25] A. Wołowicz, Z. Hubicki, The use of the chelating resin of a new generation Lewatit MonoPlus TP-220 with the bis-picolylamine functional groups in the removal of selected metal ions from acidic solutions, Chem. Eng. J. 197 (2012) 493-508.

ACCEPTED MANUSCRIPT

ACCEPTED MANUSCRIPT

[26] C. Zhu, F. Liu, C. Xu, J. Gao, D. Chen, A. Li, Enhanced removal of Cu(II) and Ni(II) from saline solution by novel dual-primary-amine chelating resin based on anion-synergism, J. Haz. Mater. 287 (2015) 234-242.

[27] G. McKay, S.J. Allen, A mathematical model for the fixed bed adsorption of Telon Blue Dye onto peat, J. Sepn. Proc. Technol., 4 (3) (1983) 8-15.

[28] B. Al Duri, B., G. McKay, Basic dye adsorption on carbon using a solid diffusion model, Chem. Eng. J. 38 (No.1) (1988) 23-32.

[29] C. Faur-Brasquet, Z. Reddad, K. Kadirvelu, P. Le Cloirec, Modeling the adsorption of metal ions (Cu^{2+}, Ni^{2+}, Pb^{2+}) onto ACCs using surface complexation models, Applied Surface Science. 196 (1–4) (2002) 356-365.

[30] J.B. Rosen, Kinetics of a fixed bed system for solid diffusion into spherical particles, J. Chem. Phys. 20 (1952) 387-392.

[31] J.B. Rosen, General numerical solution for solid diffusion in fixed beds, Ind. Eng. Chem. 46 (1954) 1590.

[32] A. Piazzoli, M. Antonelli, Application of the Homogeneous Surface Diffusion Model for the prediction of the breakthrough in full-scale GAC filters fed on groundwater, Proc. Safety Environ. Protect. 117 (2018) 286-295.

ACCEPTED MANUSCRIPT

[33] G. McKay, Solution to the homogeneous surface diffusion model for batch adsorption systems using orthogonal collocation, Chem. Eng. J. 81 (1–3) (2001) 213-221.

[34] V.K.C. Lee, G. McKay, Comparison of solutions for the homogeneous surface diffusion models applied to adsorption systems, Chem. Eng. J. 98 (3) (2004) 255-264.

[35] J.A. Nelder, R. Mead, A simplex method for function minimization, Computer Journal, 7 (1965) 308-313.

[36] J. Lehto, K. Vaaramaa, H^+/Na^+ exchange in an aminophosphonate-chelating resin, Reac. Funct. Poly. 33 (1997) 19-24.

[37] D.R. Lide, Handbook of Chemistry and Physics (79^{th} edition), Boca Raton: CRC Press, 5-93 (1998).

[38] J.E. Williamson, K.E. Bazaire, C.J. Geankoplis, Liquid mass transfer at very low Reynolds numbers, Ind. Eng. Chem. Fundam. 2 (1963) 126-129.

[39] E.J. Wilson, C.J. Geankoplis, Liquid mass transfer at very low Reynolds numbers in packed beds, Ind. Eng. Chem. Fundam. 5 (1966) 9-12.

[40] P.V. Roberts, P. Cornel, R.S. Summers, External mass transfer rate in fixed bed adsorption, J. Environ. Eng. 111 (1985) 891-905.

ACCEPTED MANUSCRIPT

[41] C.K. Ko, J.F. Porter, G. McKay, Mass transport model for the fixed bed sorption of metal ions on bone char, Ind. Eng. Chem. Res. 42 (2003) 3458-3469.

Highlights

- Removal of nickel from water by a novel Na^+/H^+ binary site ion exchange material.
- Selecting binary site resin composition based on pH change.
- Novel HSD model for binary site resin to predict nickel ion breakthrough curve.
- Effect of process variables: bed height, solution flowrate

ACCEPTED MANUSCRIPT